

Centrality Dependence of Chemical Freeze-out in Au+Au Collisions at RHIC

Masashi Kaneta¹ and Nu Xu²

¹RIKEN-BNL Research Center, Brookhaven National Laboratory, Upton, New York 11973

²Lawrence Berkeley National Laboratory, Berkeley, California 94720

(Dated: September 25, 2018)

This is a write-up of a poster presented in the international conference Quark Matter 2004 at Oakland, CA. We will report centrality dependence of chemical freeze-out temperature (T_{ch}), light quark chemical potential (μ_q), strange quark chemical potential (μ_s), and strangeness saturation factor (γ_s) in Au+Au collisions at $\sqrt{s_{NN}} = 130$ and 200 GeV. A systematic study for combination of ratios for chemical freeze-out fit is studied and we have found small combination dependences. The results show γ_s increasing with centrality but the other parameters have less sensitivity to the centralities.

PACS numbers: 25.75.-q, 24.85.+p, 13.85.-t

I. INTRODUCTION

The statistical model approach is established by analysis of particle ratios of the high energy heavy ion collisions in GSI-SIS to CERN-SPS energy [1, 2, 3, 4, 5, 6, 7] and elementary collisions (e^+e^- , pp , and $p\bar{p}$) [8, 9]. The model describes the particle ratios by the chemical freeze-out temperature (T_{ch}), the chemical potential (μ), and the strangeness saturation factor (γ_s). Many feature of the data imply that a large degree of the chemical equilibration may be reached both at AGS and SPS energies excepting strangeness hadrons. There are the four most important results.

1. At high energy collisions the chemical freeze-out (inelastic collisions cease) occurs at about 150-170 MeV and it is ‘universal’ to both elementary and the heavy ion collisions;
2. The strangeness is not fully equilibrated because γ_s is 0.5-0.8 [5, 8, 9] (if strangeness is in equilibration, $\gamma_s=1$ [1]);
3. The kinetic freeze-out (elastic scatterings cease) occurs at a lower temperature ~ 100 -120 MeV;
4. The compilation of the freeze-out parameters [10] in the heavy ion collisions in the energy range from 1 - 200 A·GeV shows that a constant energy per particle $\langle E \rangle / \langle N \rangle \sim 1$ GeV can reproduce the behavior in the temperature-potential ($T_{ch} - \mu_B$) plane [10].

We have many hadron yields and ratios including multi-strange hadrons as a function of centrality in Au+Au collisions at $\sqrt{s_{NN}} = 130$ and 200 GeV. They allow us to study centrality dependence of chemical freeze-out at RHIC energy.

II. MODEL

We adopt the grand canonical ensemble for a chemical freeze-out model based on Ref. [11] and the model used in

Ref. [12, 13, 14]. We assume no difference between u and d quark chemical potentials. Therefore, the hadron gas is described by a chemical freeze-out temperature (T_{ch}), light (u and d) quark potential (μ_q), strange quark potential (μ_s), and strangeness saturation factor (γ_s). The density of a particle i in the hadron gas is given by:

$$\rho_i = \gamma_s^{\langle s + \bar{s} \rangle_i} \frac{g_i}{2\pi^2} T_{ch}^3 \left(\frac{m_i}{T_{ch}} \right)^2 K_2(m_i/T_{ch}) \lambda_q^{Q_i} \lambda_s^{s_i} \quad (1)$$

where m_i is the mass of the hadron i , g_i is the number of spin-isospin degree-of-freedom, K_2 is the second-order modified Bessel function and,

$$\lambda_q = \exp(\mu_q/T_{ch}), \quad \lambda_s = \exp(\mu_s/T_{ch}).$$

The potential μ_q is for $u/d/\bar{u}/\bar{d}$ quarks, and μ_s is for s/\bar{s} quarks. The μ_q is a third of baryon chemical potential μ_B . Q_i and s_i correspond to the net number of valence u/d quarks ($Q_i = \langle u - \bar{u} + d - \bar{d} \rangle_i$), and s quark ($s_i = \langle s - \bar{s} \rangle_i$) of particle species i , respectively. The RHIC data we used are from mid-rapidity region, therefore we does not apply any conservation low and treat all of chemical freeze-out parameters as free parameters for the fit. The factor γ_s ($0 \leq \gamma_s$) is introduced to take account of possible incomplete chemical equilibration for strange particles [1]. $\gamma_s=1$ signifies full strangeness chemical equilibrium and $\gamma_s > 1$ shows over strangeness saturation. The power factor of γ_s is total number of s and \bar{s} quarks in the particle. It is not clear whether γ_s should be unity or not. On the other hand, calculations in Refs. [6, 14, 15, 16] support $\gamma_s < 1$. Therefore, we adopt γ_s as a free parameter. Note that we use the Boltzmann approximation for all hadrons except pions, where the Bose distribution is applied. The particle densities are computed by Eq. (1) for the hadron gas including known resonances up to mass of 1.7 GeV/ c^2 , and the effect of broad resonance mass widths is taken into account [11]. The resonance decay to lower mass hadrons after chemical freeze-out is also taken into account.

There are technical caveats in above approaches. The application of some statistical model requires that the measurement is done over the whole phase-space, *i.e.*,

with 4π particle yields. This is because conservation laws that apply to the collisions are only valid for global measurements, not locally. In all experiments the coverage of the phase-space is limited. Therefore, extracting the yields measured within limited phase-space to 4π yields is almost impossible, especially for the collider experiments. In addition, we should point out that the non-local effect is common to all global conservation laws (baryon number, charge, and so on), not only to the strangeness.

We adopt the static model that assumes full phase space to limited phase space, that is, limited rapidity region. Ref. [17] has studied effects of excluded volume correction, limited rapidity range, transverse flow, and longitudinal expansion to the ratios. Various effects which can severely distort the momentum spectra of the particles produced cancel out in such ratios [17]. This addresses that the static model can be applied to the particle ratios in the limited rapidity range.

III. ANALYSIS

Table I lists the centrality definition and references for the value of dN/dy and the ratios at mid-rapidity for each experiment. The centralities are defined by the independent detector and different acceptances among the experiments. The common parameter of the collision centrality is an average of number of participant ($\langle N_{part} \rangle$). Therefore, we use $\langle N_{part} \rangle$ to discuss the centrality dependence of the chemical freeze-out parameters.

We select two kind of centrality binning from STAR data. The first one is used for data set from charged pion, kaon and proton (centrality selection used in Ref. [27, 29] for 130 GeV and Ref. [38] for 200 GeV). The second one has smaller number of bins but more particle ratios (centrality selection used in Ref. [22] for 130 GeV and Ref. [40] for 200 GeV). The other experiments have different centrality bins, therefore we need to estimate particle ratio for the centrality bins selected. At first, we interpolate the dN/dy of each particle assuming linear scaling of $\langle N_{part} \rangle$ between two data points. After we obtained dN/dy values for the $\langle N_{part} \rangle$, the particle ratios is computed from the dN/dy values.

The chemical freeze-out model fit is applied to the particle ratios. A program package MINUIT [43] is used for the fit to find χ^2 minimum points and the error of fit parameters is estimated as χ^2 minimum + 1. The chemical freeze-out parameters seem to be sensitive to combination of particle ratios as discussed in Ref. [14]. Hence we check the following six combinations of particle ratios for the fit: (1) π , K , and p ; (2) π , K , p and Λ ; (3) π , K , p , Λ , ϕ , and Ξ ; (4) π , K , p , Λ , K^* , ϕ , and Ξ ; (5) π , K , p , Λ , ϕ , Ξ , and Ω ; (6) π , K , p , Λ , K^* , ϕ , Ξ , and Ω .

TABLE I: List of possible dN/dy and ratios from the experimental data in the Au+Au collisions at $\sqrt{s_{NN}} = 130$ GeV and 200 GeV. The parenthetic particle name ($\langle K^{*0} \rangle$ and $\langle K^\pm \rangle$) means average of the particle and the anti-particle. The selection of event fraction is defined by (I) the multiplicity of charged particles from the Multiplicity Array [18], (II) the energy deposit on Zero Degree Calorimeter (ZDC) and the number of charged particle measured by Beam-Beam Counter (BBC) [19], (III) the signal of the scintillator paddle counters [20], (IV) the energy deposit on ZDC and the signal of Central Trigger Barrel (CTB) [21], (V) the number of reconstructed charged tracks ($\eta < |0.75|$) [22], (VI) the number of reconstructed charged tracks ($\eta < |0.5|$). Additionally, some references show the number of participant and the dN/η of negative charged hadrons for the event fraction. We marked them in the list by $\langle N_{part} \rangle$ and $dN_{h^-}/d\eta$.

$\sqrt{s_{NN}}$	experiment	Refs.	dN/dy or ratio	centrality presented
130 GeV	BRHAMS	[23]	π^-/π^+	(I) $\langle N_{part} \rangle$
		[23]	\bar{p}/p	(I) $\langle N_{part} \rangle$
	PHENIX	[24, 25]	π^+, π^-	(II) $\langle N_{part} \rangle$
		[24, 25]	K^+, K^-	(II) $\langle N_{part} \rangle$
		[24, 25]	p, \bar{p}	(II) $\langle N_{part} \rangle$
		[25]	$\Lambda, \bar{\Lambda}$	(II) $\langle N_{part} \rangle$
	PHOBOS	[26]	π^-/π^+	(III) $\langle N_{part} \rangle$
		[26]	K^-/K^+	(III) $\langle N_{part} \rangle$
		[26]	\bar{p}/p	(III) $\langle N_{part} \rangle$
	STAR	[21]	π^-	(IV) $\langle N_{part} \rangle$ $dN_{h^-}/d\eta$
		[27]	K^+, K^-, K_S^0	(V) $dN_{h^-}/d\eta$
		[28]	\bar{K}^{*0}/K^{*0}	(IV)
		[28]	$\langle K^{*0} \rangle$	(IV)
		[29]	\bar{p}	(V)
		[30]	\bar{p}/p	(V)
		[31]	ϕ	(V)
		[22]	$\Lambda, \bar{\Lambda}$	(VI)
		[32, 33]	$\Xi^-, \bar{\Xi}^+$	(V)
		[33, 34]	$\Omega^-, \bar{\Omega}^+$	(V)
200 GeV	BRAHMS	[35]	π^-/π^+	(I) $\langle N_{part} \rangle$
		[35]	K^-/K^+	(I) $\langle N_{part} \rangle$
		[35]	\bar{p}/p	(I) $\langle N_{part} \rangle$
	PHOBOS	[36]	π^-/π^+	(III) $\langle N_{part} \rangle$
		[36]	K^-/K^+	(III) $\langle N_{part} \rangle$
		[36]	\bar{p}/p	(III) $\langle N_{part} \rangle$
	PHENIX	[37]	π^+, π^-	(II) $\langle N_{part} \rangle$
		[37]	K^+, K^-	(II) $\langle N_{part} \rangle$
		[37]	p, \bar{p}	(II) $\langle N_{part} \rangle$
	STAR	[38]	π^+, π^-	(VI) $\langle N_{part} \rangle$
		[38]	K^+, K^-	(VI) $\langle N_{part} \rangle$
		[38]	p, \bar{p}	(VI) $\langle N_{part} \rangle$
		[39]	$\langle K^{*0} \rangle/\langle K^\pm \rangle$	(VI)
		[40]	ϕ	(VI)
		[41]	$\Lambda + \bar{\Lambda}$	(VI)
	[42]		$\Xi^-, \bar{\Xi}^+$	(VI)
	[34]		$\Omega^-, \bar{\Omega}^+$	(VI)

IV. RESULTS AND DISCUSSION

Figure 1 shows centrality dependence of chemical freeze-out temperature T_{ch} , light-quark potential μ_q (= $\mu_B/3$ where μ_B is Baryonic chemical potential), strange

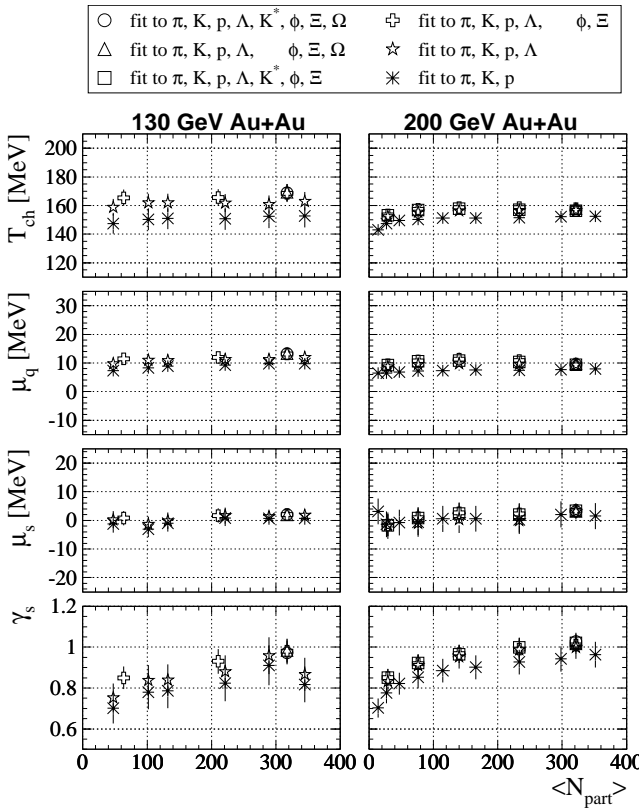


FIG. 1: Chemical freeze-out temperature T_{ch} , light-quark potential μ_q , strange quark potential μ_s , and strangeness saturation factor γ_s as a function of $\langle N_{part} \rangle$ in 130 and 200 GeV Au+Au collisions. The markers correspond to combination of ratios used for fit as shown in the figure. Table II lists all of values shown in Fig. 1.

quark potential μ_s , and strangeness saturation factor γ_s as a function of $\langle N_{part} \rangle$ in 130 and 200 GeV Au+Au collisions. The markers correspond to combination of ratios used for fit as shown in the figure. Table II lists all of values shown in Fig. 1.

The chemical freeze-out parameters vary with combination of particle ratios and shows larger variation in 130 GeV Au+Au than 200 GeV. Taking care the variation, T_{ch} , μ_q , and μ_s seems to be constant with centrality in both 130 GeV and 200 GeV Au+Au collisions. The γ_s is slightly increasing with centrality in 130 GeV when we focus the results by the fit to ratio from π , K , p , Λ , K^* , ϕ , Ξ (,and Ω). On the other hand, we can see the rise of γ_s as a function of $\langle N_{part} \rangle$ in any combination of ratios in 200 GeV Au+Au. The γ_s is about 0.5~0.7 in the heavy ion collisions at SPS energies [16], e^+e^- at LEP, and $p\bar{p}$ at SppS [8, 9]. Only Au+Au central collisions at RHIC energy ($\sqrt{s_{NN}} = 130$ and 200 GeV) reach fully strangeness equilibration. The rise of γ_s seems to be rapid until around $\langle N_{part} \rangle = 100$ -150 and then slowly increasing.

The T_{ch} , μ_q , μ_s seem to be independent as a function of $\langle N_{part} \rangle$. Within errors and the variation of results from combination dependence, T_{ch} is 150–170 MeV, μ_q

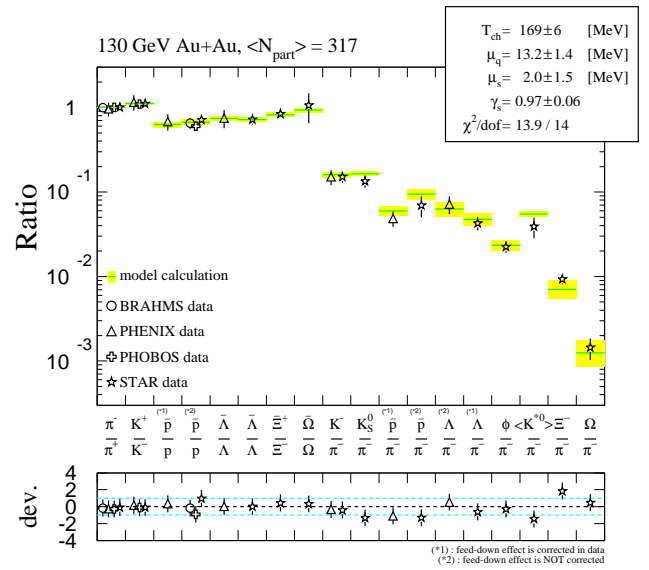


FIG. 2: Comparison of fit results to the data in 130 GeV Au+Au central collisions ($\langle N_{part} \rangle = 317$). All of data from dataset (6) shown in the plot are used for the fit. The point with marker is experimental data. In the top plot, the model calculations of ratio from the chemical freeze-out parameters obtained are shown horizontal line. The variation in the error of the parameters is shown as shaded box. The bottom plot shows a deviation of data to the model, $(r_{exp} - r_{model})/\Delta r_{exp}$, where r_{exp} is ratio from data, r_{model} is ratio by model calculation, and Δr_{exp} is error of r_{exp} .

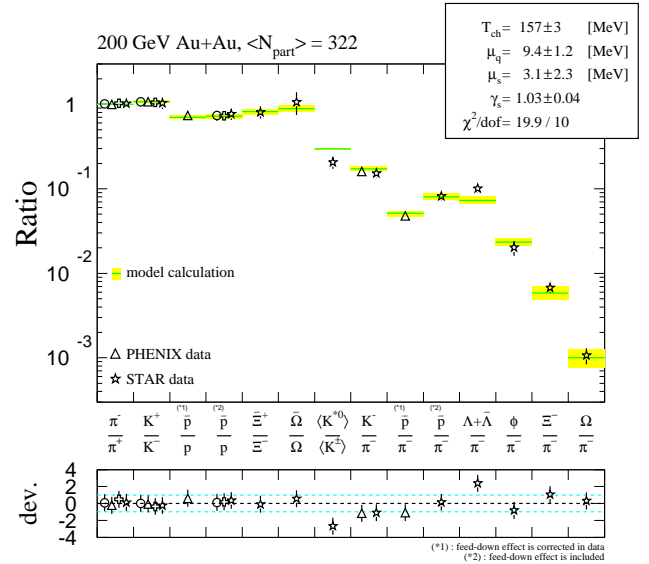


FIG. 3: Comparison of fit results to the data in 200 GeV Au+Au central collisions ($\langle N_{part} \rangle = 322$). All of data from dataset (6) shown in the plot are used for the fit. The legend is the same with Fig. 2.

is 8–11 MeV, and μ_s is -3–3 MeV. Small but finite μ_q reflects net baryon density is small but not zero around mid-rapidity. The μ_s is consistent with zero. It suggests that the chemical freeze-out occurs at phase boundary of a hadron gas.[1, 44, 45].

The chemical freeze-out parameter varies by data combination. In the central 130 GeV Au+Au data, T_{ch} , μ_q , μ_s , and γ_s change about 10 MeV, 4MeV, 1MeV and 0.1, respectively. The deviation is small and consistent within error for all of parameters. The variation becomes smaller in the central 200 GeV Au+Au data. It is about 5 MeV, 2MeV, 2MeV and 0.06 for T_{ch} , μ_q , μ_s , and γ_s , respectively. The results from both energy shows that the γ_s increases when we adopt multi-strangeness in the fit at a centrality bin. The γ_s is sensitive to multi-strangeness, therefore the constrain changes stronger with increasing number of strangeness data point in the fit. However, it is not clear how the number of strangeness play the role in the constrain. We need to check this point with more data that will come soon from RHIC run4.

Figure 2 and 3 show a comparison of data to the model calculation. The data is included multi-strangeness and it is all of possible data sample at this time (dataset (6)). The model calculation shows good agreement in both energy, excepting K^* . In the 200GeV, the $(\Lambda + \bar{\Lambda})/\pi^-$ value from model also differ to the data. Note that the data $\Lambda + \bar{\Lambda}$ is obtained from a slide of the conference presen-

tation from Ref. [41] and the value seems to be changed in Quark Matter 2004 conference, therefore the results might be changed and we need to check in future.

V. SUMMARY

We study centrality dependence of chemical freeze-out parameters in $\sqrt{s_{NN}} = 130$ and 200 GeV Au+Au collisions. The T_{ch} , μ_q , μ_s show independence as a function of $\langle N_{part} \rangle$. The most remarkable point is about centrality dependence of γ_s . The result shows γ_s increasing with centrality and reach fully strangeness equilibration in only Au+Au central collisions at RHIC energy. The rise of γ_s seems to be rapid until around $\langle N_{part} \rangle = 100$ -150 and then slowly increasing. The ratio combination dependence is also studied in both energy and we have found small combination dependences. The T_{ch} , μ_q , μ_s seem to be independent as a function of $\langle N_{part} \rangle$. On the other hand, the γ_s increases when we adopt multi-strangeness in the fit at a centrality bin.

Acknowledgments

We thank Jean Cleymans for useful discussion.

[1] J. Rafelski, Phys. Lett. **B262**, 333 (1991).
 [2] P. Braun-Munzinger, J. Stachel, J. Wessels, and N. Xu, Phys. Lett. **B344**, 43 (1995).
 [3] J. Cleymans, D. Elliott, H. Satz, and R. Thews, Z. Phys. **C319**, 1 (1997).
 [4] P. Braun-Munzinger, J. Stachel, J. Wessels, and N. Xu, Phys. Lett. **B365**, 1 (1996).
 [5] A. Panagiotou, G. Mavromanolakis, and J. Tzoulis, Phys. Rev. **C53**, 1353 (1996).
 [6] J. Letessier and J. Rafelski, J. Phys. **G25**, 295 (1999).
 [7] J. Cleymans, H. Oeschler, and K. Redlich, Phys. Rev. **C59**, 1663 (1999).
 [8] F. Becattini, Z. Phys. **C69**, 485 (1996).
 [9] F. Becattini and U. Heinz, Z. Phys. **C76**, 269 (1997).
 [10] J. Cleymans and K. Redlich, Phys. Rev. Lett. **59**, 5284 (1998).
 [11] J. Sollfrank, U. Heinz, H. Sorge, and N. Xu, Phys. Rev. **C59**, 1637 (1999).
 [12] M. Kaneta and N. Xu, J. Phys. **G27**, 589 (2001).
 [13] N. Xu and M. Kaneta, Nucl. Phys. **A698**, 306c (2002).
 [14] I. G. Bearden et al. (NA44), Phys. Rev. **C66**, 044907 (2002).
 [15] F. Becattini, J. Cleymans, A. Keränen, E. Suhonen, and K. Redlich, Phys. Rev. **C64**, 024901 (2001).
 [16] F. Becattini, M. Gaździcki, and J. Sollfrank, Eur. Phys. J. **C5**, 143 (1998).
 [17] J. Cleymans, H. Oeschler, and K. Redlich, J. Phys. **G25**, 281 (1999).
 [18] I. G. Bearden et al. (BRAHMS), Phys. Lett. **B523**, 227 (2001), nucl-ex/0108016.
 [19] K. Adcox et al. (PHENIX), Phys. Rev. Lett. **86**, 3500 (2001).
 [20] B. B. Back et al. (PHOBOS), Phys. Rev. Lett. **85**, 3100 (2000).
 [21] M. Calderon de la Barca Sanchez et al. (STAR) (2001), nucl-ex/0110009.
 [22] C. Adler et al. (STAR), Phys. Rev. Lett. **89**, 092301 (2002), nucl-ex/0203016.
 [23] I. G. Bearden et al. (BRAHMS), Phys. Rev. Lett. **87**, 112305 (2001).
 [24] K. Adcox et al. (PHENIX), Phys. Rev. Lett. **88**, 242301 (2002).
 [25] K. Adcox et al. (PHENIX), Phys. Rev. Lett. **89**, 092302 (2002), nucl-ex/0204007.
 [26] B. B. Back et al. (PHOBOS), Phys. Rev. Lett. **87**, 102301 (2001).
 [27] C. Adler et al. (STAR) (2002), nucl-ex/0206008.
 [28] C. Adler et al. (STAR), Phys. Rev. **C66**, 061901 (2002).
 [29] C. Adler et al. (STAR), Phys. Rev. Lett. **87**, 262302 (2001), nucl-ex/0110009.
 [30] C. Adler et al. (STAR), Phys. Rev. Lett. **86**, 4778 (2001).
 [31] C. Adler et al. (STAR), Phys. Rev. **C65**, 041901(R) (2002).
 [32] J. Castillo et al. (STAR) (2002), nucl-ex/0210032.
 [33] J. Adams et al. (STAR) (2003), nucl-ex/0307024.
 [34] C. Suire et al. (STAR) (2002), nucl-ex/0211017.
 [35] I. G. Bearden et al. (BRAHMS) (2002), nucl-ex/0207006.
 [36] B. Wosiek et al. (PHOBOS) (2002), nucl-ex/0210037.
 [37] S. S. Adler et al. (PHENIX) (2003), nucl-ex/0307022.
 [38] J. Adams et al. (STAR) (2003), nucl-ex/0310004.

TABLE II: Chemical freeze-out parameters for each average number of participant ($\langle N_{part} \rangle$). The data set is related to combination of ratios used for the fit: (1) π , K , and p ; (2) π , K , p and Λ ; (3) π , K , p , Λ , ϕ , and Ξ ; (4) π , K , p , Λ , K^* , ϕ , and Ξ ; (5) π , K , p , Λ , ϕ , Ξ , and Ω ; (6) π , K , p , Λ , K^* , ϕ , Ξ , and Ω . The parameters are obtained by fit of chemical freeze-out model to the data. The error of parameters are defined as χ^2 minimum + 1.

Collision system	Data set	$\langle N_{part} \rangle$	T_{ch} [MeV]	μ_q [MeV]	μ_s [MeV]	γ_s	χ^2/N_{dof}
130 GeV Au+Au	(1)	345	152.8 \pm 8.0	9.8 \pm 1.9	0.7 \pm 2.1	0.817 \pm 0.088	0.9/ 4
		289	152.4 \pm 8.1	9.7 \pm 1.9	0.7 \pm 2.2	0.911 \pm 0.098	0.5/ 4
		221	150.8 \pm 7.7	9.3 \pm 1.9	0.8 \pm 2.8	0.824 \pm 0.088	1.1/ 4
		132	151.1 \pm 7.7	8.8 \pm 1.8	-0.9 \pm 2.9	0.786 \pm 0.084	1.9/ 4
		102	150.2 \pm 7.4	8.3 \pm 1.8	-3.0 \pm 2.7	0.780 \pm 0.083	1.5/ 4
		48	147.3 \pm 6.9	7.3 \pm 2.0	-1.1 \pm 3.1	0.701 \pm 0.075	1.9/ 4
	(2)	345	162.9 \pm 6.5	11.9 \pm 1.8	1.8 \pm 2.0	0.867 \pm 0.081	4.5/ 8
		289	160.7 \pm 6.2	11.2 \pm 1.7	1.3 \pm 2.1	0.958 \pm 0.090	2.9/ 8
		221	161.7 \pm 6.4	11.3 \pm 1.8	1.7 \pm 2.7	0.879 \pm 0.081	5.4/ 8
		132	161.9 \pm 6.3	10.8 \pm 1.8	0.0 \pm 2.8	0.840 \pm 0.077	6.3/ 8
		102	162.1 \pm 6.3	11.0 \pm 1.8	-1.3 \pm 2.7	0.837 \pm 0.076	7.6/ 8
		48	158.8 \pm 5.9	9.7 \pm 1.9	0.3 \pm 3.0	0.753 \pm 0.069	9.4/ 8
	(3)	317	168.6 \pm 6.1	13.2 \pm 1.4	2.0 \pm 1.5	0.980 \pm 0.059	11.5/ 11
		211	165.6 \pm 5.9	11.9 \pm 1.8	1.7 \pm 2.5	0.930 \pm 0.060	8.4/ 11
		64	165.5 \pm 5.6	11.5 \pm 1.8	0.8 \pm 2.5	0.850 \pm 0.055	17.2/ 11
	(5)	317	169.2 \pm 6.0	13.2 \pm 1.4	1.9 \pm 1.5	0.984 \pm 0.057	11.7/ 13
	(6)	317	169.1 \pm 6.1	13.2 \pm 1.4	2.0 \pm 1.5	0.972 \pm 0.057	13.9/ 14
200 GeV Au+Au	(1)	351	152.4 \pm 3.3	7.9 \pm 2.1	1.5 \pm 4.6	0.963 \pm 0.063	1.2/ 3
		298	152.1 \pm 3.3	7.7 \pm 2.0	2.1 \pm 4.6	0.942 \pm 0.062	1.1/ 3
		234	151.6 \pm 3.2	7.4 \pm 2.0	0.3 \pm 4.6	0.927 \pm 0.060	1.4/ 3
		166	151.2 \pm 3.2	7.6 \pm 2.0	0.6 \pm 4.5	0.902 \pm 0.059	1.9/ 3
		115	151.2 \pm 3.2	7.3 \pm 2.0	0.6 \pm 4.5	0.884 \pm 0.058	2.3/ 3
		76	150.3 \pm 3.1	7.2 \pm 2.0	-0.5 \pm 4.5	0.853 \pm 0.056	3.1/ 3
		47	149.5 \pm 3.1	6.8 \pm 2.0	-0.6 \pm 4.5	0.822 \pm 0.054	4.9/ 3
		27	147.4 \pm 2.9	6.4 \pm 2.0	-1.3 \pm 4.5	0.776 \pm 0.051	7.2/ 3
		14	143.1 \pm 2.7	6.5 \pm 2.0	3.1 \pm 4.5	0.702 \pm 0.047	11.4/ 3
	(2)	322	156.5 \pm 2.9	9.3 \pm 1.2	3.0 \pm 2.6	0.999 \pm 0.056	10.3/ 4
		234	156.5 \pm 3.5	9.6 \pm 2.4	0.0 \pm 4.7	0.987 \pm 0.059	13.1/ 4
		140	156.3 \pm 3.6	9.7 \pm 2.4	0.3 \pm 4.7	0.952 \pm 0.057	15.1/ 4
		76	155.3 \pm 3.5	9.5 \pm 2.4	-0.9 \pm 4.7	0.910 \pm 0.055	16.5/ 4
		29	152.4 \pm 3.3	8.7 \pm 2.3	-1.8 \pm 4.7	0.833 \pm 0.050	20.6/ 4
	(3)	322	157.8 \pm 2.7	9.7 \pm 1.2	3.5 \pm 2.4	1.011 \pm 0.044	12.1/ 7
		234	158.5 \pm 3.2	10.9 \pm 2.2	2.3 \pm 3.8	0.990 \pm 0.046	14.4/ 7
		140	158.6 \pm 3.2	11.4 \pm 2.2	2.6 \pm 3.6	0.968 \pm 0.045	16.9/ 7
		76	157.2 \pm 3.0	10.8 \pm 2.1	0.9 \pm 3.6	0.920 \pm 0.042	17.4/ 7
		29	153.4 \pm 2.9	9.3 \pm 2.1	-1.5 \pm 3.8	0.850 \pm 0.043	21.1/ 7
	(4)	322	156.3 \pm 2.7	9.4 \pm 1.2	3.4 \pm 2.4	1.020 \pm 0.045	19.5/ 8
		234	157.2 \pm 3.1	10.3 \pm 2.1	2.0 \pm 3.7	0.999 \pm 0.046	19.3/ 8
		140	157.8 \pm 3.0	10.9 \pm 2.1	2.5 \pm 3.6	0.965 \pm 0.044	18.6/ 8
		76	156.8 \pm 3.0	10.6 \pm 2.1	0.9 \pm 3.6	0.922 \pm 0.042	18.3/ 8
		29	153.2 \pm 2.8	9.2 \pm 2.1	-1.6 \pm 3.8	0.852 \pm 0.043	21.4/ 8
	(5)	322	157.9 \pm 2.7	9.7 \pm 1.2	3.2 \pm 2.3	1.016 \pm 0.042	12.5/ 9
	(6)	322	156.5 \pm 2.6	9.4 \pm 1.2	3.1 \pm 2.3	1.027 \pm 0.043	19.9/ 10

- [39] H. Zhang et al. (STAR) (2003), nucl-ex/0306034.
- [40] E. Yamamoto et al. (STAR), Nucl. Phys. **A715**, 466c (2003).
- [41] H. Long et al. (STAR) (2003), Slide on SQM2003 web page : <http://www.phy.duke.edu/SQM2003/>.
- [42] J. Castillo et al. (STAR) (2003), Slide on HIC03 web page : <http://www.physics.mcgill.ca/HIC03/>.
- [43] F. James, *MINUIT - Function Minimization and Error Analysis. Reference Manual*, CERN, Geneva (1984).
- [44] K. Lee, M. Rhoades-Brown, and U. Heinz, Phys. Rev. **C37**, 1452 (1988).
- [45] M. Asprouli and A. Panagiotou, Phys. Rev. **D51**, 1086 (1995).